https://doi.org/10.5194/essd-2023-335
Preprint. Discussion started: 24 August 2023

Open Access Earth System Science Data Discussions

An 800-kyr planktonic $\delta^{18}O$ stack for the West Pacific Warm Pool

Christen L. Bowman[1], Devin S. Rand[1], Lorraine E. Lisiecki[1], and Samantha C. Bova[2]

[1]Department of Earth Science, University of California Santa Barbara, Santa Barbara, CA, 93106, USA

[2]Department of Geological Sciences, San Diego State University, San Diego, CA, 92182, USA

Correspondence to: Lorraine E. Lisiecki (lisiecki@geol.ucsb.edu)

Abstract. The West Pacific Warm Pool (WPWP) exhibits different glacial-interglacial climate variability than high latitudes, and its sea surface temperatures are thought to respond primarily to changes in greenhouse gas. To better characterize the orbital scale climate response of the WPWP, we constructed a planktonic $\delta^{18}O$ stack (average) of 11 previously published WPWP records of the last 800 kyr, available at https://doi.org/10.5281/zenodo.8190829 (Bowman et al., 2023), using new Bayesian alignment and stacking software BIGMACS. Similarities in stack uncertainty between the WPWP planktonic $\delta^{18}O$ stack and benthic $\delta^{18}O$ stacks also constructed using BIGMACS demonstrate that the software performs similarly well when aligning regional planktonic or benthic $\delta^{18}O$ data. Sixty-seven radiocarbon dates from four of the WPWP cores suggest that WPWP planktonic $\delta^{18}O$ change is nearly synchronous with global benthic $\delta^{18}O$ during the last glacial termination. However, the WPWP planktonic $\delta^{18}O$ stack exhibits less glacial/interglacial amplitude and less spectral power at all orbital frequencies than benthic $\delta^{18}O$. We assert that the WPWP planktonic $\delta^{18}O$ stack provides a useful representation of orbital-scale regional climate response and a regional alignment target, particularly for the higher resolution 0 - 450 ka portion of our stack.

1 Introduction

The tropical Pacific is an important source of heat and moisture to the atmosphere and is thought to have a strong impact on global climate responses during glacial cycles (Lea et al., 2000). Prior studies suggest that the climate of the West Pacific Warm Pool (WPWP), which is defined by mean annual sea surface temperatures (SST) above 28°C, responds primarily to changes in greenhouse gas concentrations due to the region's large distance from high-latitude ice sheets (Lea, 2004; Tachikawa et al., 2014). Additionally, Earth's orbital cycles cause seasonal variations in insolation (i.e., incoming solar radiation), which affect Earth's high and low latitudes differently, with only 0.3°C of WPWP SST change attributed to orbital forcing during the Late Pleistocene (Tachikawa et al., 2014). Thus, climate records of the WPWP region are expected to have features which differ from many other locations on Earth. Here we seek to characterize WPWP climate on orbital timescales and its differences from high-latitude climate, which can help test hypotheses about the sensitivity of the WPWP to orbital forcing, ice volume, and greenhouse gas concentration.

One of the most commonly used paleoceanographic climate proxies is the ratio of oxygen isotopes, denoted as $\delta^{18}O$, in calcium carbonate from foraminiferal shells; this proxy is affected by both water temperature and the $\delta^{18}O$ of seawater,

https://doi.org/10.5194/essd-2023-335
Preprint. Discussion started: 24 August 2023


Open Access Earth System Science Data Discussions

which varies with global ice volume as well as local salinity. The two general types of foraminifera are benthic and planktonic, which live in the deep ocean and surface ocean, respectively. Benthic $\delta^{18}O$ is considered a high-latitude climate proxy because deep water temperature is set in high-latitude deep water formation regions and because global ice volume responds primarily to high-latitude northern hemisphere summer insolation. However, planktonic $\delta^{18}O$ is influenced by both high-latitude ice volume and local SST and salinity. Previous studies from the WPWP have shown smaller glacial-interglacial amplitudes of planktonic $\delta^{18}O$ change than in benthic $\delta^{18}O$ or planktonic $\delta^{18}O$ from other regions. This difference has been attributed to smaller sea surface temperature fluctuations and salinity changes in the WPWP (Lea et al., 2000). Here we present a stack (time-dependent average) of planktonic $\delta^{18}O$ records from eleven cores across the WPWP to provide a record of its regional responses over the past 800 kyr, which can be compared to the high-latitude response of global benthic $\delta^{18}O$ stacks.

The new planktonic $\delta^{18}O$ stack of the WPWP region presented here is intended to better characterize orbital responses in WPWP planktonic $\delta^{18}O$ and to improve age models for WPWP sediment cores. Age models for ocean sediment cores, which provide estimates of sediment age as a function of core depth, are commonly constructed by stratigraphic correlation (i.e., alignment) of an individual core's $\delta^{18}O$ record to a global $\delta^{18}O$ stack such as the LR04 or SPECMAP stacks (Linsley and Breymann, 1991; Lea et al, 2000; Chuang et al., 2018; Lisiecki and Raymo, 2005; Imbrie et al., 1984). A stack is the time-dependent average of data from multiple ocean sediment cores that share a common climatic signal, thus increasing the signal-to-noise ratio of the data. Traditionally, stacks have been constructed from global compilations of benthic $\delta^{18}O$ (Lisiecki and Raymo, 2005), planktonic $\boldsymbol{\delta}^{18}O$ (Shakun et al., 2015) or a combination of the two (Imbrie et al., 1984; Huybers and Wunsch, 2004). However, recent studies have advocated the development of regional stacks (Lisiecki and Stern, 2016; Lee and Rand et al., accepted) to distinguish spatial differences in the timing and amplitude of $\delta^{18}O$ changes.

We constructed a WPWP planktonic $\delta^{18}O$ stack spanning 0-800 kyr using new Bayesian alignment and stacking software, BIGMACS (Lee and Rand et al., accepted). The new stack consists of previously published planktonic $\delta^{18}O$ data from eleven tropical Western Pacific cores and 67 radiocarbon dates between 0-43 kyr BP from four of the cores. Here we present the new WPWP stack and a brief comparison of orbital power in the new stack compared to the LR04 global benthic $\delta^{18}O$ stack (Lisiecki and Raymo, 2005) and a recently published stack of WPWP SST (Jian et al., 2022). We also evaluate the relative timing of WPWP planktonic $\delta^{18}O$ change versus benthic $\delta^{18}O$ change during the last glacial termination (T1).

2 Study Area

The West Pacific Warm Pool is a region of the equatorial Pacific with annual average SST between 28°C to 30°C. It covers an area between approximately 15 degrees S to 15 degrees N and 115 to 160 degrees E (Locarnini et al., 2018), with boundaries defined by mean annual SST of greater than 28°C (Tachikawa et al., 2014). Synchronous change in $\delta^{18}O$ is

https://doi.org/10.5194/essd-2023-335
Preprint. Discussion started: 24 August 2023

assumed for the cores that are stacked, so homogeneous conditions in the core locations are important for maintaining the accuracy of the stack. The largely homogeneous WPWP surface ocean makes it a suitable choice for stacking (Lea et al., 2000; Li et al., 2011).

However, our new stack includes two cores just beyond the boundary of the typically defined WPWP region. We choose to include these cores because their high resolution records extend the full length of the stack, and they exhibit oceanographic variability broadly comparable to that observed within the warm pool proper over the period of interest. Core ODP-1143 from the South China Sea, which lies just beyond the northwestern border of the modern WPWP, has an average annual temperature of ~28°C and receives northward flowing water from the WPWP during summer (Li et al., 2011). Core MD05-2930 is located along the southern limit of the WPWP in the Gulf of Papua; its SST is primarily controlled by the Australasian Monsoon, with modern SST fluctuating between 26°C - 29°C (Regoli et al., 2015). The slightly cooler sea surface temperatures of these two cores are expected to yield slightly more positive $\delta^{18}O$ values than other WPWP sites and may be affected by orbital-scale changes in the WPWP extent.

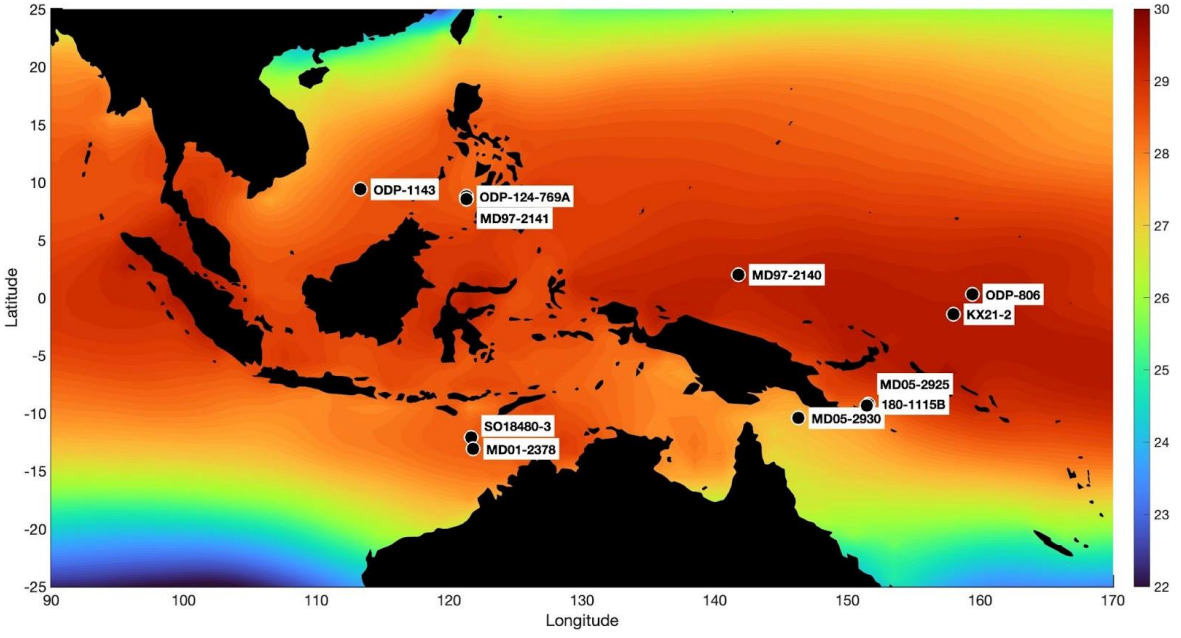

Figure 1. Core locations and mean annual sea surface temperatures (°C, color) from 1955-2018 (Locarnini et al., 2018).

3 Data

We compiled from the scientific literature $\delta^{18}O$ measurements of planktonic foraminifera from eleven tropical Western Pacific cores in or near the WPWP (**Table 1**). Six of the cores extend back to 300-500 ka, and five span the last 750 kyr (**Fig.**

https://doi.org/10.5194/essd-2023-335
Preprint. Discussion started: 24 August 2023

2). All but one core in the stack uses $\delta^{18}O$ values measured from the planktonic species *Globigerinoides ruber (G. ruber)* sensu stricto (s.s.), whose depth habitat is the upper 30m of the mixed layer (Wang, 2000). One core, 180-1115B, has data from a different planktonic species, *Globigerinoides sacculifer (G. sacculifer)* whose depth habitat is 20-75m (Sadekov et al., 2009). A species correction of -0.11‰ was applied to the *G. sacculifer* data according to the values presented by Spero et al. (2003).

A total of 5569 planktonic $\delta^{18}O$ measurements were used to create the stack. The stack spans 0 - 800 ka; however, there is a significant decrease in data density from 450-800 ka. Only five cores extend beyond 450 ka, and this portion of the stack is composed of only 833 data points. The lower data resolution results in greater uncertainty and smoothness for the $\delta^{18}O$ features in the older portion of the stack; therefore, we focus our analysis of the stack on the first 450 kyr.

The stacking algorithm counts each $\delta^{18}O$ measurement equally, so cores with higher resolution have more influence on the stack. The mean sample spacing of the core data used to create the stack ranges from 0.33-3.9 kyr, with lower average sample spacing for the long cores that extend to the older half of the stack. Although the published data for core MD97-2141 has a mean sample spacing of 0.11 kyr, we smoothed the data using a 3-point running mean and reduced its mean sample spacing to 0.33 kyr, so that it does not overly dominate the regional stack. Additionally, we constrain the stack age model using 67 previously published radiocarbon measurements ranging from 0.89 ka to 43.46 ka from four cores (Holbourn et al., 2005; Jian et al., 2022; Lo et al., 2017; Regoli et al., 2015).

Table 1. Locations of cores in the WPWP stack and the temporal coverage of their planktonic $\delta^{18}O$ data.

Core	Latitude	Longitude	Oldest Age (ka)	Avg Resolution (kyr)	Original Publication
ODP806	0.30	159.40	469.1	2.30	Lea et al., 2000
ODP124-769A	8.79	121.29	774.1	1.22	Linsley and Breymann, 1991
ODP1143	9.40	113.30	798.3	1.83	Li et al., 2011
180-1115B	-9.19	151.57	798.7	2.24	Chuang et al., 2018
MD97-2141	8.80	121.30	395.6	0.33[b]	Oppo et al., 2003
MD97-2140	2.00	141.80	797.2	3.90	de Garidel-Thoron et al., 2005
MD05-2930 [a]	-10.42	146.30	799.7	2.03	Regoli et al., 2015
MD05-2925 [a]	-9.34	151.46	462.7	0.76	Lo et al., 2017
KX21-2	-1.42	157.98	394.5	0.93	Dang et al., 2020
MD01-2378 [a]	-13.08	121.79	459.6	1.08	Holbourn et al., 2005
SO18480-3 [a]	-12.09	121.65	307.0	0.43	Jian et al., 2022

[a] indicates core with radiocarbon data, [b] indicates new resolution after smoothing and subsampling

https://doi.org/10.5194/essd-2023-335
Preprint. Discussion started: 24 August 2023

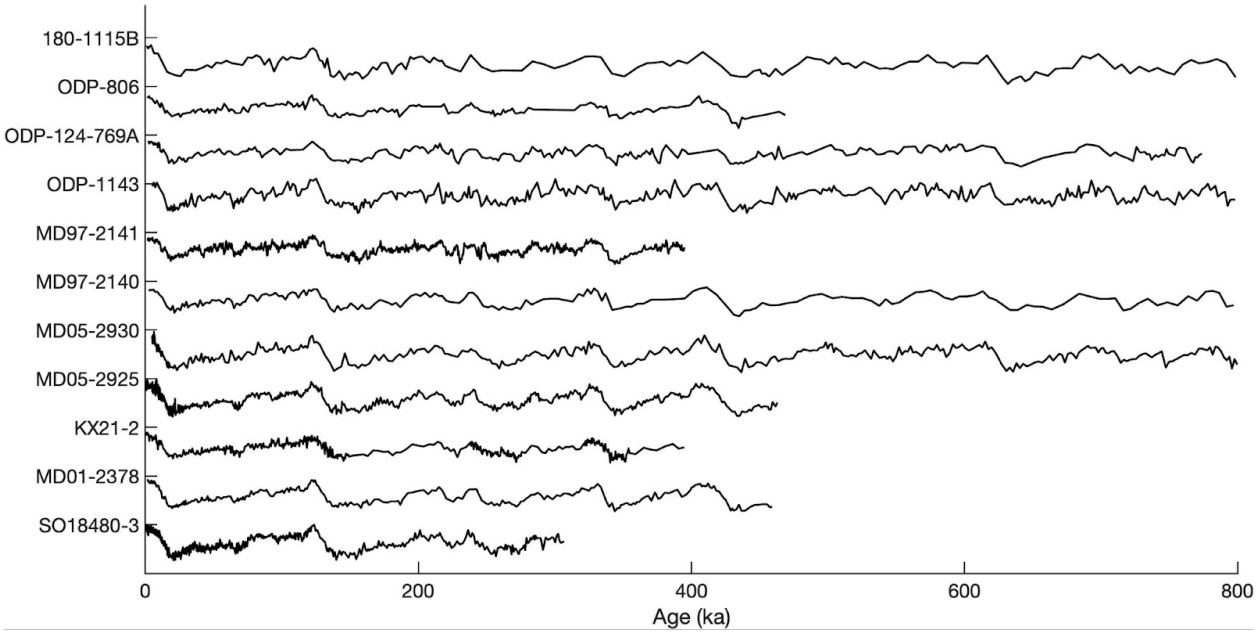

Figure 2. Planktonic $\delta^{18}O$ data of the cores used in the WPWP stack construction, plotted on BIGMACS age model for each core and offset vertically. Data are from sites 180-1115B (Chuang et al., 2018),ODP-806 (Lea et al., 2000), ODP-124-769A (Linsley and Breymann, 1991), ODP-1143 (Li et al., 2011), MD97-2141 (Oppo et al., 2003), MD05-2140 (de Garidel-Thoron et al., 2005), MD05-2930 (Regoli et al., 2015), MD05-2925 (Lo et al., 2017), KX21-2 (Dang et al., 2020), MD01-2378 (Holbourn et al., 2005), and SO18480-3 (Jian et al., 2022).

4 Methods

4.1 Stack Construction

We use the new Bayesian software package BIGMACS to construct the planktonic $\delta^{18}O$ WPWP stack (Lee and Rand et al., accepted). BIGMACS, which stands for Bayesian Inference Gaussian process regression and Multiproxy Alignment for Continuous Stacks, constructs multiproxy age models and stacks by combining age information from both direct age constraints (e.g., radiocarbon data) and probabilistic alignments of $\delta^{18}O$ to a target record. Although BIGMACS was developed for benthic $\delta^{18}O$, here we use BIGMACS to align and stack planktonic $\delta^{18}O$; thus, we present analysis to verify the performance of the software for this new application.

BIGMACS stack construction is an iterative process with two steps. In the first step, age models are estimated for each record by aligning to an initial target. Each $\delta^{18}O$ record is shifted and scaled to better match the target stack during alignment and likelihoods assigned to age estimates for each core depth are based on residuals between the core's $\delta^{18}O$ value and the

https://doi.org/10.5194/essd-2023-335
Preprint. Discussion started: 24 August 2023

target's time-dependent mean and standard deviation. The shift/scale values represent how each core was adjusted to better match the alignment target. During alignment, shift and scale parameters are learned to correct for differences in species and latitudes. BIGMACS updates its alignment parameters using the Expectation Maximization (EM) algorithm to maximize likelihood. Core sites with homogeneous planktonic $\delta^{18}O$ values to have shift parameters close to 0 and scale parameters close to 1. In the second step, a stack is constructed using the age models. The new stack is then used as the alignment target to construct age models for the next iteration. Iterations are performed until convergence.

The initial alignment target we used for constructing the WPWP stack was the LR04 stack of 57 globally distributed benthic $\delta^{18}O$ records (Lisiecki and Raymo, 2005) with a constant standard deviation of 0.5‰. The original age model for the LR04 stack was created by orbital tuning to a simple ice volume model and has estimated age uncertainties of +/- 4 kyr for the past 800 kyr, i.e., time range of the WPWP stack (Lisiecki and Raymo, 2005). Despite the age uncertainty of the LR04 stack and the fact that it reflects benthic rather than planktonic $\delta^{18}O$, it was chosen as the initial alignment target because it is a widely used age model that spans the full 800 kyr of the new WPWP stack.

The first 43 ka Before Present (BP) of the WPWP is constrained by 67 radiocarbon dates from four cores. We calibrated radiocarbon ages using the Marine20 calibration curve (Heaton et al., 2020), a reservoir age offset of 0 kyr, and reservoir age standard deviations of 0.2 kyr. Ages for the remainder of the stack are largely determined by the timing of glacial cycles in the LR04 stack. Thus, the timing of planktonic $\delta^{18}O$ change in the WPWP stack is assumed to be synchronous with the LR04 benthic stack. In section 6.1, we show that there is strong agreement between the timing of planktonic and benthic $\delta^{18}O$ change in the WPWP stack and the LR04 stack during the first 43 ka BP in which WPWP ages are predominantly determined by radiocarbon data.

Core age models were also constrained by age estimates for the first and last $\delta^{18}O$ measurement from each core based on previous publications. Age uncertainty for these estimates were assigned a Gaussian distribution with a standard deviation of 4 kyr. Lastly, tie points were included for cores ODP-180-1115B at 75 ka, MD97-2141 at 63 ka and 92.5 ka, and SO18480-3 at 75 ka to improve the alignment of Marine Isotope Stages (MIS) 3 and 4. These tie points were assigned a Gaussian distribution with a standard deviation of 1 kyr.

4.2 Conversions of SST and sea level to isotopic equivalents

To compare the amplitude of WPWP planktonic $\delta^{18}O$ change with the ice volume (sea level) and WPWP SST changes that affect planktonic $\delta^{18}O$, we convert a sea level record and WPWP SST stack to the amount of $\delta^{18}O$ change they are expected to cause. The global sea level stack of Spratt and Lisiecki (2016) was used to calculate an equivalent change in $\delta^{18}O$ due to ice volume ($\Delta\delta^{18}O_{ice}$) using a conversion of 0.009‰ per meter of sea level. This conversion represents the long-term average effect of ice volume change because the size of the effect varies slightly depending on the average $\delta^{18}O$ composition of the ice (Spratt and Lisiecki, 2016).

https://doi.org/10.5194/essd-2023-335
Preprint. Discussion started: 24 August 2023

The WPWP SST stack from Jian et al. (2022) was converted to an $\delta^{18}O$ equivalent using Eq. (1):

$$\Delta\delta^{18}O_{SST} = \frac{-1(SST-29)}{4.8} \quad (1)$$

The 4.8 scaling factor was presented by Bemis et al. (1998). A shift of 29 was chosen to express the effects of SST change relative to a modern WPWP mean SST of 29. Thus, the resulting $\Delta\delta^{18}O_{SST}$ measures change relative to the present day.

4.3 Spectral Analysis

Power spectral density was calculated to quantify the strengths of response to orbital frequencies in $\delta^{18}O$ for our WPWP and the LR04 stacks (Lisiecki and Raymo, 2005). Power spectral density was calculated from a Fast Fourier Transform (FFT) with the number of frequencies set to 1024. Frequencies corresponding to the orbital cycle lengths of eccentricity (100 kyr), obliquity (41 kyr), and precession (23 and 19 kyr) are of particular interest to see how the insolation changes from the cycles affect the $\delta^{18}O$ values.

Normalized power spectral density was also calculated for the WPWP SST stack and our WPWP $\delta^{18}O$ stack from 0-360 ka to match the age range of the SST stack (Jian et al., 2022). The power spectral density of each record was normalized by dividing by the maximum peak height of the dominant ~100 kyr glacial cycle to evaluate the relative strength of different orbital frequencies.

5 Results

The probabilistic stack created by BIGMACS models the $\delta^{18}O$ value at any point in time as a Gaussian distribution with a time-varying mean and standard deviation. BIGMACS also estimates and applies shift and scale parameters for each core to optimize fit with the stack (Table 2). The standard deviation of the stack reflects scatter in the shifted-and-scaled $\delta^{18}O$ measurements at each point in time, including the effects of uncertainty in each core's $\delta^{18}O$ alignment to the stack. The standard deviation of the stack does not include any information about absolute age uncertainty. However, uncertainty does increase where data are more sparse. The standard deviation of the new WPWP planktonic $\delta^{18}O$ stack has an average value of 0.20‰ for the full stack and 0.18‰ for 0-450 ka, where data coverage is most dense.

https://doi.org/10.5194/essd-2023-335
Preprint. Discussion started: 24 August 2023

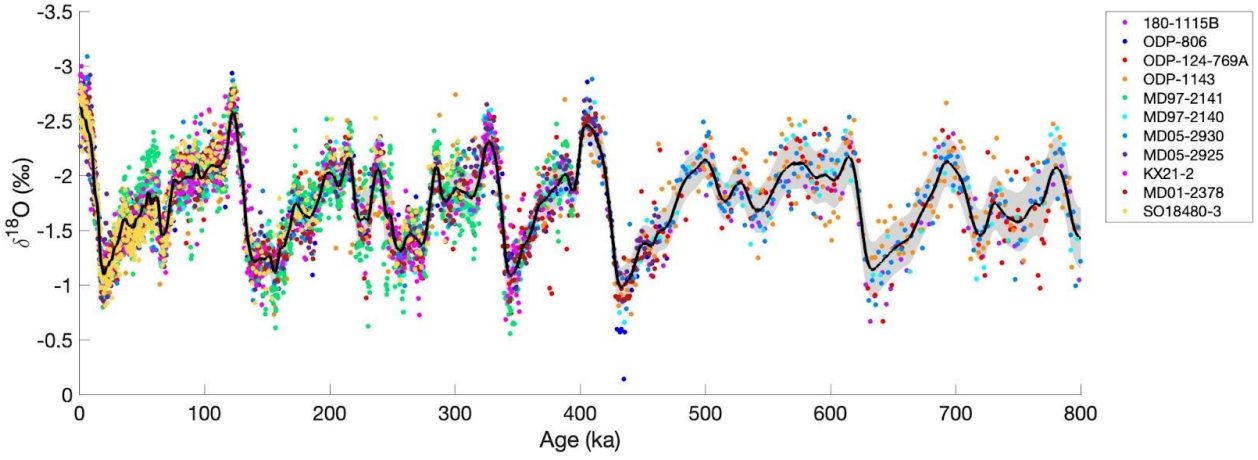

Figure 3. The WPWP planktonic δ^{18}O stack mean (black) and 1 standard deviation (gray shading). Colored dots show the planktonic δ^{18}O measurements from each core after applying the core-specific shift and scale parameters calculated during alignment. Data from MD97-2141 was smoothed and sampled at one-third the originally published resolution.

Table 2. Shift and scale values for each core in the WPWP stack.

Core	Shift	Scale
KX21-2	-0.26764	0.80483
ODP-806	-0.33788	0.72619
ODP-1143	-0.44173	1.0404
ODP-124-769A	-0.54915	0.78291
MD97-2141	-0.62289	0.7725
MD97-2140	-0.26955	0.88078
MD05-2930	0.46154	1.0864
MD05-2925	0.2283	1.0861
180-1115B	0.56016	1.0785
MD01-2378	0.03179	1.0036
SO18480-3	0.088366	1.0913

https://doi.org/10.5194/essd-2023-335
Preprint. Discussion started: 24 August 2023

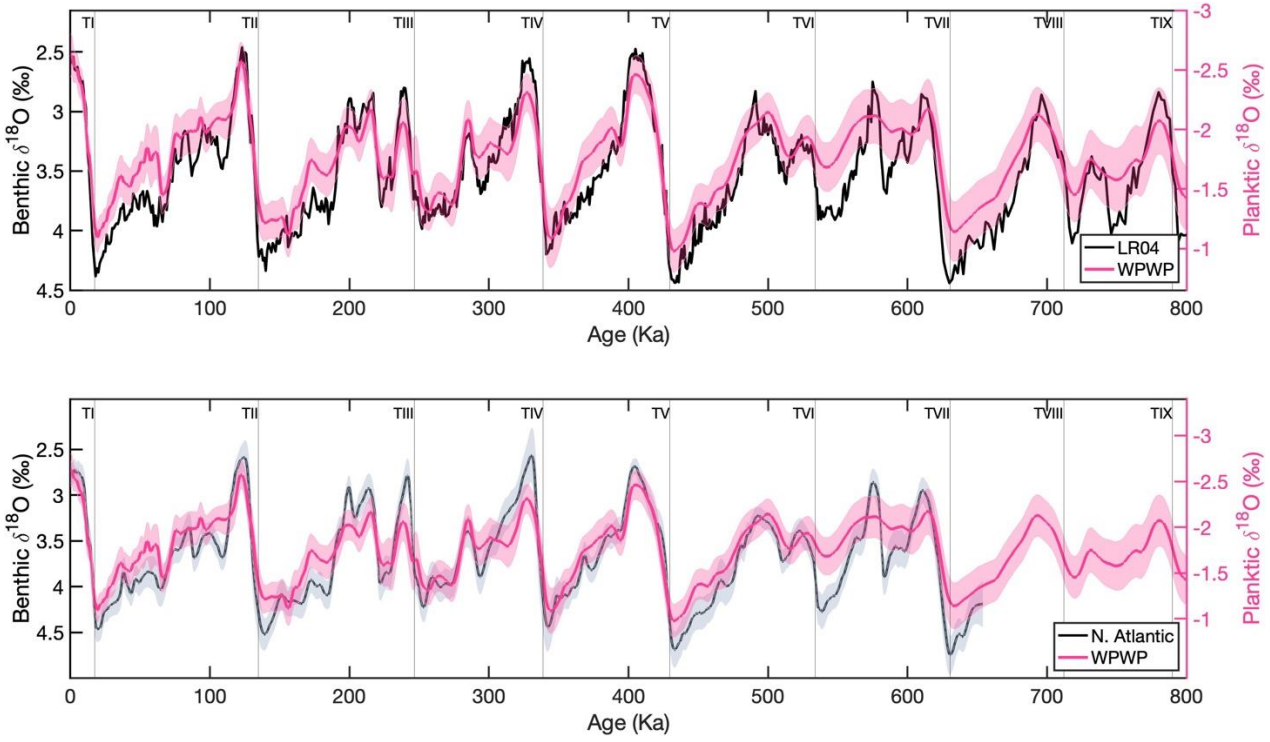

Figure 4. Stack comparisons. (top) Comparison between our WPWP planktonic $\delta^{18}O$ stack (pink) and the global benthic $\delta^{18}O$ LR04 stack (black) (Lisiecki and Raymo, 2005). (bottom) Comparison between our planktonic $\delta^{18}O$ WPWP stack (pink) and a regional North Atlantic benthic $\delta^{18}O$ stack (black) (Hobart et al., 2023). Shaded error bars represent one standard deviation in the WPWP and North Atlantic stacks. Glacial terminations are labelled with vertical lines based on ages for TI - TVII from Hobart et al. (2023); and TVIII-TIX from Lisiecki and Raymo (2005).

The planktonic WPWP stack has a weaker the glacial-interglacial amplitude than the LR04 and North Atlantic benthic $\delta^{18}O$ stacks. The average glacial/interglacial amplitude for Terminations I - V is 1.7‰ and 1.8‰ in the LR04 and North Atlantic benthic stacks, respectively, but only 1.3‰ in the WPWP planktonic stack. This amplitude difference is also reflected in the spectral analysis of the stacks. Across all three orbital frequencies, there is greater spectral power in the benthic LR04 stack than the planktonic WPWP stack (**Fig. 5)**. The total variance in the LR04 stack from 0-800 ka is 0.1256‰^{2} whereas the total WPWP variance is only 0.0694‰^{2}.

https://doi.org/10.5194/essd-2023-335
Preprint. Discussion started: 24 August 2023

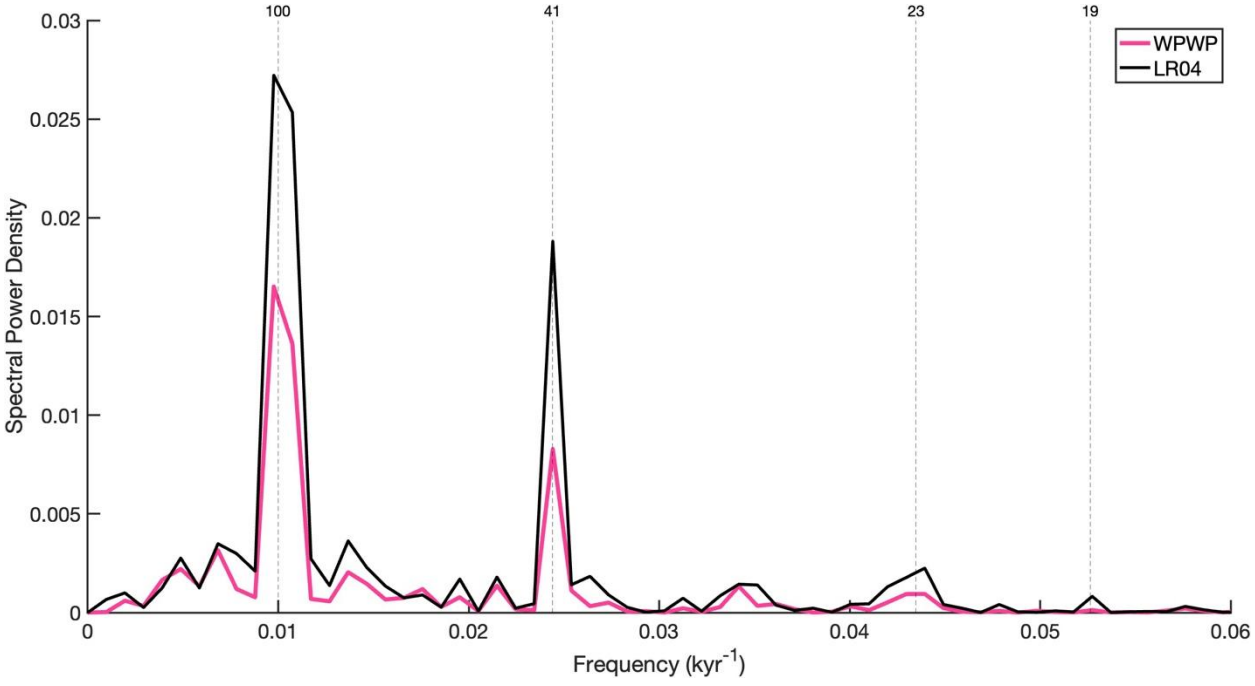

Figure 5. Spectral power density of our planktonic δ^{18}O WPWP stack (pink) and the LR04 benthic δ^{18}O stack (black). Spectral power is calculated from 0-800 ka for both stacks. Orbital frequencies that correspond to 100, 41, 23 and 19 kyr are labeled with vertical dashed lines.

6 Methods validation and limitations

6.1 Age Model Assumptions

The use of the LR04 stack as an initial alignment target for our WPWP stack assumes benthic and planktonic δ^{18}O are changing synchronously; however, the signals recorded by benthic and planktonic δ^{18}O could differ in timing due to either transit time of the global ice volume signal to the deep ocean compared to surface of the tropical West Pacific and/or due to asynchronous temperature and salinity changes between the WPWP and high-latitude deep water formation regions. To evaluate potential timing differences in the two signals, we compare the age model for the portion of the WPWP planktonic stack constrained by radiocarbon data (0 - 43 ka BP) to the equivalent portion of the benthic LR04 and LS16 global benthic δ^{18}O stacks (Lisiecki and Raymo, 2005; Lisiecki and Stern, 2016). The LS16 global stack is constructed with direct ^{14}C age constraints and is weighted towards the Pacific based on ocean basin volume, whereas the LR04 stack is based only on indirect age constraints and more heavily weighted toward Atlantic values (Lisiecki and Raymo, 2005; Lisiecki and Stern, 2016). However, all three age models show good agreement for the timing of δ^{18}O change during Termination I, suggesting that age estimates for WPWP planktonic and benthic δ^{18}O are similar on orbital time scales (**Fig. 6**).

https://doi.org/10.5194/essd-2023-335
Preprint. Discussion started: 24 August 2023

The relative timing of millennial-scale variability between the WPWP planktonic stack and benthic $\delta^{18}O$ is more difficult to evaluate. Apparent differences in timing of a millennial-scale feature in the stacks between 36-38 ka may be an artifact of age model uncertainty. Age uncertainty for the LR04 stack beyond 30 ka is ± 4 kyr, and age estimates for the LS16 stack have a 95% confidence interval width of 2-4 kyr between 30-40 ka. Age estimates for that portion of our WPWP stack are not well constrained due to the scarcity of radiocarbon samples available beyond 30 ka. The portions of our WPWP stack older than 45 ka, which are not constrained by radiocarbon data, inherit the +/- 4 kyr age uncertainty of the LR04 stack used as the initial alignment target. Thus, we have no independent age estimates for WPWP planktonic $\delta^{18}O$ changes older than 45 ka.

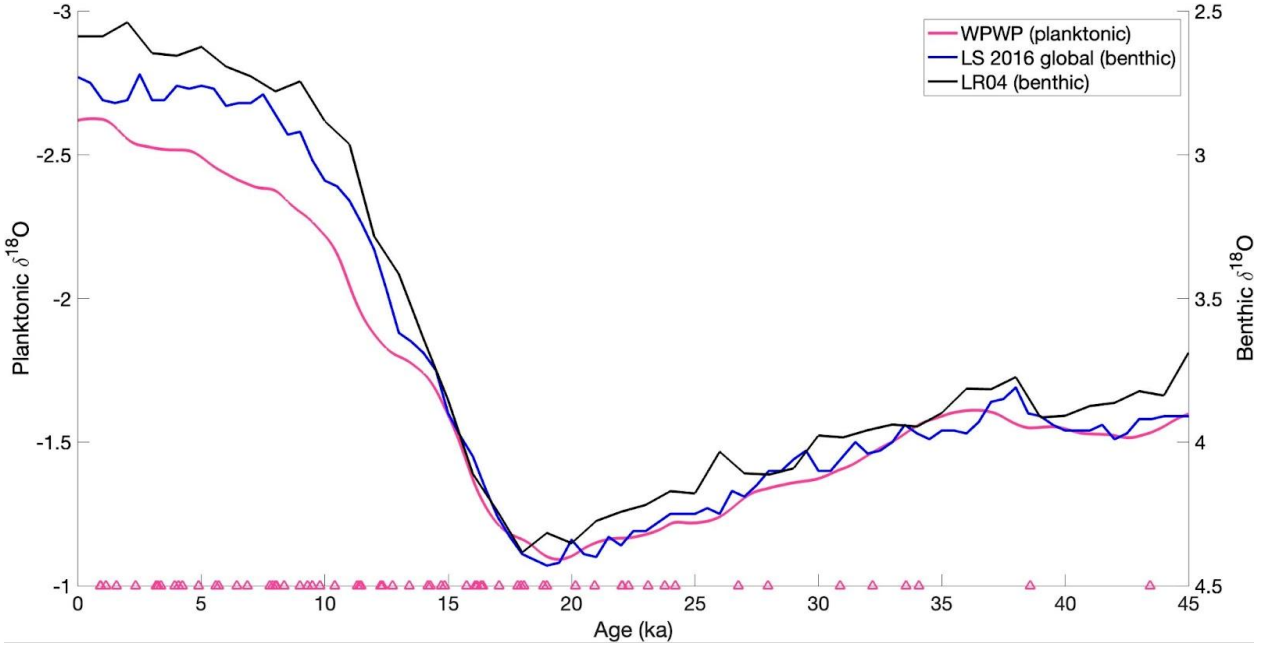

Figure 6. Our WPWP planktonic $\delta^{18}O$ stack (pink) compared to the global benthic $\delta^{18}O$ stacks of Lisiecki and Stern (2016) (blue) and Lisiecki and Raymo (2005) (black). Triangles represent radiocarbon ages included in our WPWP stack construction (Holbourn et al., 2005; Jian et al., 2022; Lo et al., 2017; Regoli et al., 2015).

6.2 Application of BIGMACS to Planktonic $\delta^{18}O$

6.2.1 Standard Deviation of Planktonic Versus Benthic Stacks

The new Bayesian alignment software BIGMACS has previously only been applied to benthic $\delta^{18}O$ data (Lee and Rand et al., accepted), and this study is the first to use the software to stack planktonic $\delta^{18}O$ data. To evaluate the performance of BIGMACS in stacking benthic and planktonic $\delta^{18}O$, we compare the standard deviation of the new WPWP planktonic $\delta^{18}O$

https://doi.org/10.5194/essd-2023-335
Preprint. Discussion started: 24 August 2023

stack to benthic $\delta^{18}O$ stacks constructed with BIGMACS using six cores from the Deep Northeast Atlantic (DNEA stack) and four cores from the Intermediate Tropical Western Atlantic (ITWA stack). A similar standard deviation for $\delta^{18}O$ in the stacks would indicate a similar signal-to-noise ratio in the stacked data, suggesting a similar effectiveness in the stacking process.

The DNEA and ITWA stacks have standard deviations of 0.13‰ and 0.2‰, respectively, for 0 - 60 ka (Lee and Rand et al., accepted), while our WPWP planktonic stack has a mean standard deviation of 0.15‰ for the same age range. A larger mean standard deviation of 0.20‰ for the full age range of 0 - 800 ka for our WPWP stack is likely due in part to the lower resolution of data used in the second half of the stack; however, it is still similar to the standard deviation of the ITWA benthic stack. The similar $\delta^{18}O$ standard deviations for the planktonic and benthic stacks suggests that BIGMACS may be similarly effective at aligning and stacking homogeneous regional planktonic $\delta^{18}O$ data as regional benthic data. However, before stacking either benthic or planktonic $\delta^{18}O$ records, BIGMACS users should carefully evaluate whether the records to be aligned and stacked are homogeneous (i.e., share a common and synchronous signal).

6.2.2 Homogeneity of WPWP Planktonic $\delta^{18}O$

The process of stack construction assumes that all WPWP planktonic $\delta^{18}O$ records used have one homogeneous signal, but physical processes, such as temperature and salinity gradients, could create variation between the WPWP core locations. The shift and scale values calculated for each record during stack construction can be used as an estimate of how similar or different the means and amplitudes of the planktonic $\delta^{18}O$ signals are between cores. The shift values of the 11 cores in the WPWP stack range between -0.62 and 0.56 ‰, and scale values adjust the amplitudes of the signals by a factor of 0.72 - 1.09 (Table 2). The benthic DNEA and ITWA stacks constructed using BIGMACS have a smaller range of shift and scale parameters than the WPWP stack, with shift values ranging from -0.07 to 0.25 ‰ and -0.25 to 0.3 ‰ for the DNEA and ITWA stacks, respectively (Lee and Rand et al., accepted). Benthic scale values vary between 0.92 to 1.04 for the DNEA and 0.91 to 1 for the IWTA (Lee and Rand et al., accepted). Thus, the shift and scale values suggest more spatial variability in WPWP planktonic $\delta^{18}O$ than in regional benthic $\delta^{18}O$ compilations.

WPWP cores ODP-124-769A and MD97-2141, both of which are located in the Sulu Sea, have two of the most negative shifts and smallest scale values (Linsley et al., 1991; Oppo et al., 2003). Cores KX21-2 and ODP-806, located in the eastern, open ocean portion of the WPWP, also have small scale values and negative shifts (Dang et al., 2020**;** Lea et al., 2000). The similar shift and scale values for pairs of neighboring cores with different data resolution suggest that these results reflect real differences in SST or salinity variability within the WPWP and indicate a weaker amplitude for planktonic $\delta^{18}O$ change at these sites. Previous studies show regional differences in $\delta^{18}O_{seawater}$ that may explain the reduced amplitude of planktonic $\delta^{18}O$ change at sites in the Sulu Sea and eastern WPWP (de Garidel-Thoron et al., 2005). Unlike the central and southern

https://doi.org/10.5194/essd-2023-335
Preprint. Discussion started: 24 August 2023

WPWP where glacial surface water $\delta^{18}O$ was more positive at the LGM (Visser et al., 2003; Xu et al., 2008, Li et al. 2016), these sites show negative shifts in surface water $\delta^{18}O$ at the LGM (Rosenthal et al., 2003; Lea et al., 2000). The observed heterogeneity in $\delta^{18}O_{seawater}$ likely results from regional differences in precipitation (de Garidel-Thoron et al., 2005) and/or the varied impacts of changes in sea level on the Indonesian throughflow and connectivity of regional seas (Linsley et al., 2010).

Although alignment of $\delta^{18}O$ signals for stacking requires an assumption that the WPWP planktonic $\delta^{18}O$ is homogenous, the BIGMACS estimated core-specific shift and scale parameters should allow us to still extract the underlying signal common to the region despite small differences in the mean and amplitude of the signal among core sites. The similar standard deviation for the planktonic stack compared to benthic stack suggests that the shift and scale factors are effective for identifying a common, shared planktonic $\delta^{18}O$ signal across the WPWP.

More variability in the planktonic data is expected because the surface ocean composition has greater spatial variability due to factors like temperature and salinity than the deep ocean, which could account for some of the disparity in shift and scale values of the benthic versus planktonic data. The greater spatial variability in planktonic data is one reason why regional planktonic stacks would be more useful than global planktonic stacks. By describing regional patterns of response, regional planktonic stacks can improve age models based on stratigraphic alignment. The higher resolution, 0 - 450 ka portion of our WPWP stack may be particularly useful for this purpose. Although the new WPWP planktonic stack can improve estimates of relative age regionally, we caution that its absolute ages are susceptible to our assumption of synchronous change in benthic $\delta^{18}O$ and WPWP planktonic $\delta^{18}O$ and the absolute age uncertainty of the LR04 stack.

6.2.3 Planktonic vs. Benthic Alignment Uncertainty

Here we evaluate whether the spatial variability of WPWP planktonic $\delta^{18}O$ and its amplitude lead to systematic differences in the uncertainty of core alignments for planktonic versus benthic stack construction. The average 95% confidence interval width for alignment uncertainty across all WPWP cores is 4.8 kyr for the full length of the WPWP stack and 4.4 kyr for the 0-450 kyr portion of the stack, which has higher resolution data. Similarly, a North Atlantic benthic $\delta^{18}O$ stack also constructed using BIGMACS has an average alignment uncertainty of 4.4 kyr for the 0 - 654 ka length of that stack (Hobart et al., 2023). Thus, we find that BIGMACS alignment uncertainty for WPWP planktonic $\delta^{18}O$ is similar to the uncertainty associated with benthic $\delta^{18}O$ stack construction.

6.3 Contributions of SST and Ice Volume to WPWP Planktonic $\delta^{18}O$

A recent study by Jian et al. (2022) constructed a WPWP SST stack from 0-360 ka. We compare the orbital-scale variability between the SST stack and our planktonic $\delta^{18}O$ stack using spectral analysis and by converting the SST stack change to

https://doi.org/10.5194/essd-2023-335
Preprint. Discussion started: 24 August 2023

Open Access Earth System Science Data Discussions

$\Delta\delta^{18}O_{SST}$, which is an estimate of the oxygen isotope fractionation in foraminiferal carbonate caused by SST. Many of the same features can be seen the WPWP stacks of planktonic $\delta^{18}O$ and SST (**Fig. 7,** upper panel); however, the planktonic $\delta^{18}O$ values of the last two interglacials are similar to one another whereas SST for the Holocene is notably cooler than for the penultimate interglacial. The WPWP planktonic $\delta^{18}O$ and SST stacks have similar proportions of spectral power at orbital frequencies, but SST has slightly less 41kyr obliquity power (**Fig. 8).**

To estimate the combined effects of SST and ice volume change, the WPWP $\Delta\delta^{18}O_{SST}$ was added to an estimate of $\Delta\delta^{18}O_{ice}$ (**Fig. 7, bottom**) from a global sea level (ice volume) stack (Spratt and Lisiecki, 2016). The combined SST and ice volume $\Delta\delta^{18}O_{SST+ice}$ should represent the majority of the planktonic $\delta^{18}O$ change in our WPWP planktonic $\delta^{18}O$ stack, except for salinity-induced changes. The two combined $\Delta\delta^{18}O$ components show similar glacial/interglacial cyclicity and timing of change as our WPWP planktonic $\delta^{18}O$ stack but with a slightly larger amplitude, particularly during MIS 2-3 (20-70 ka), MIS 7 (200-250 ka) and MIS 9 (310-330 ka). Salinity-induced changes in the $\delta^{18}O$ of WPWP surface water may offset some of the WPWP $\Delta\delta^{18}O_{SST+ice}$ signal. However, some of the discrepancy could also be explained by spatial variability in the WPWP if the sites used for our planktonic $\delta^{18}O$ stack had less average SST change than those in the SST stack (Jian et al., 2022).

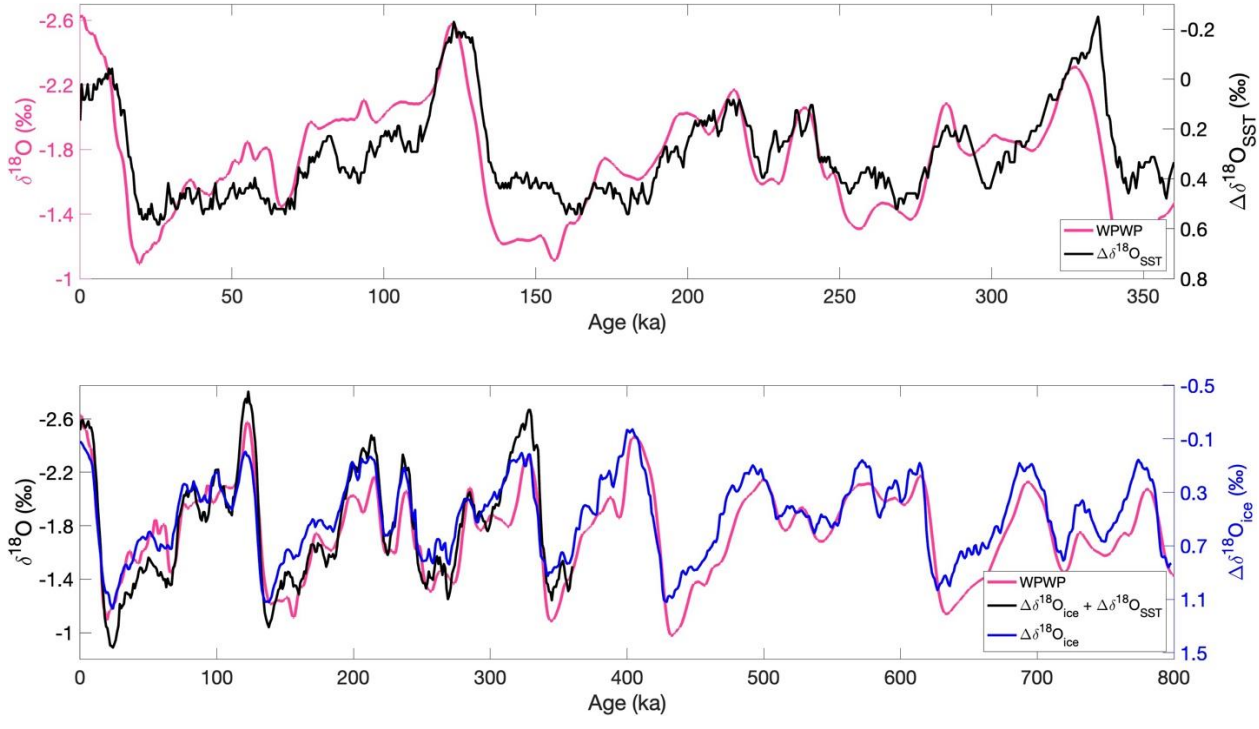

Figure 7. Contributions to WPWP planktonic $\delta^{18}O$. (top) The WPWP planktonic $\delta^{18}O$ stack (pink) and the WPWP SST stack of Jian et al. 2022, on its original age model and converted to Δ $\delta^{18}O$ per mil-equivalent (black). (bottom) The WPWP stack (pink) compared to a

https://doi.org/10.5194/essd-2023-335
Preprint. Discussion started: 24 August 2023

sea level stack (Spratt and Lisiecki, 2016) converted to $\Delta\delta^{18}O_{ice}$ per mil-equivalent (blue), and the sum of $\Delta\delta^{18}O_{SST}$ and $\Delta\delta^{18}O_{ice}$ change (black).

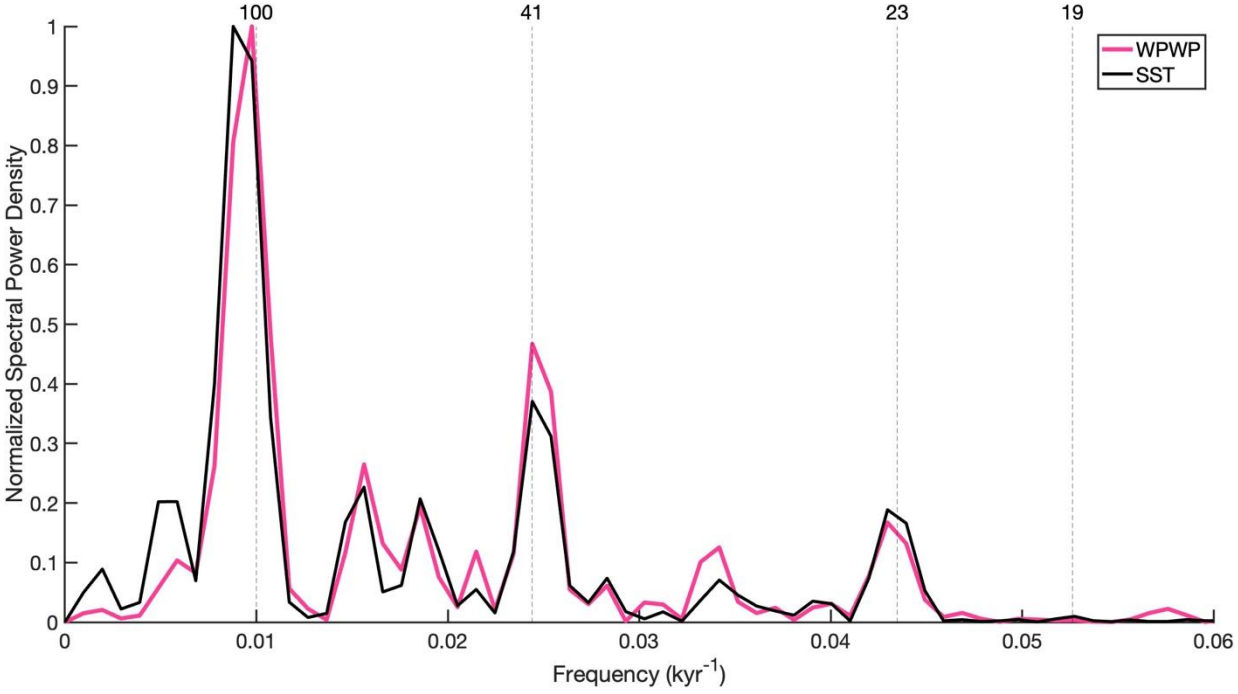

Figure 8. Normalized power spectral density of the WPWP planktonic $\delta^{18}O$ stack (pink) and WPWP SST stack (black, Jian et al., 2022) from 0-360 ka for both stacks. Orbital frequencies that correspond to 100, 41, 23 and 19 kyr are marked by vertical dashed lines.

7 Data Availability

The WPWP planktonic $\delta^{18}O$ stack can be accessed on Zenodo with the DOI https://doi.org/10.5281/zenodo.8190829 (Bowman et al., 2023) in the "WPWP_planktonic_stack.txt" file, which contains the age, mean $\delta^{18}O$, and the $\delta^{18}O$ standard deviation. The same file is also available as "stack.txt" in the 'Output' folder. The previously published depth and planktonic $\delta^{18}O$ data as well as any radiocarbon or tie points for each core used during stack construction can be found as .txt files in the 'Inputs' folder. BIGMACS produced age models, depth, and planktonic $\delta^{18}O$ data for each core can be found in the 'Outputs' folder in the "results.mat" file and as .txt files in the individual folders named for each core.

The alignment software BIGMACS used to construct our WPWP stack can be downloaded at the following DOI: https://github.com/eilion/BIGMACS (Lee and Rand et al., accepted).

https://doi.org/10.5194/essd-2023-335
Preprint. Discussion started: 24 August 2023

8 Conclusions

We present a regional planktonic $\delta^{18}O$ stack of the West Pacific Warm Pool constructed from eleven previously published cores using the new alignment software BIGMACS (Lee and Rand et al., accepted). The stack age model is constrained by 67 radiocarbon dates from 0.89 - 43.46 ka BP in four WPWP cores and otherwise follows the age model of the LR04 benthic $\delta^{18}O$ stack (Lisiecki and Raymo, 2005). Within the radiocarbon time interval, the timing of WPWP planktonic $\delta^{18}O$ appears nearly synchronous with global mean benthic $\delta^{18}O$ change. The WPWP planktonic $\delta^{18}O$ stack provides a useful regional alignment target for WPWP planktonic $\delta^{18}O$ records, particularly for the 0 - 450 ka portion which is higher resolution than the older portion of the stack. Future improvements to the WPWP stack could include higher resolution planktonic $\delta^{18}O$ in the older portion of the stack and more age constraints beyond 25 ka BP.

Analyses of the stack's standard deviation and alignment uncertainty suggest that BIGMACS performs similarly well stacking WPWP planktonic $\delta^{18}O$ as it does for regional benthic $\delta^{18}O$ data. The new stack demonstrates weaker glacial/interglacial amplitudes and orbital power for WPWP planktonic $\delta^{18}O$ change than benthic $\delta^{18}O$ stacks over the last 800 kyr. WPWP planktonic $\delta^{18}O$ change is also somewhat weaker than estimated based on global ice volume and WPWP SST change, perhaps due to spatial heterogeneity or surface salinity change.

Author Contribution

CLB curated the previously published data, performed the formal analysis, visualization, and prepared the original draft. DSR was involved with age model methodology/software development and manuscript review and editing. LEL conceptualized the project, supervised, and contributed to the original draft preparation and manuscript review and editing. SCB provided validation and manuscript review and editing.

Competing Interests

The authors declare that they have no conflict of interest.

Acknowledgments

This work was supported in part by the National Science Foundation (NSF) under the project number OCE-1760878.

References

Bemis, B. E., Spero, H. J., Bijma, J., Lea, D. W.: Reevaluation of the oxygen isotopic composition of planktonic foraminifera: Experimental results and revised paleotemperature equations, Paleoceanogr., 13(2), 150-160, https://doi.org/10.1029/98PA00070, 1998.

https://doi.org/10.5194/essd-2023-335
Preprint. Discussion started: 24 August 2023

Bowman, C. L., Rand, D. S., Lisiecki, L. E., Bova, S. C.: An 800 kyr planktonic $\boldsymbol{\delta}^{18}$O stack for the West Pacific Warm Pool, Zeodo [data set], https://doi.org/10.5281/zenodo.8190829, 2023.

Channell, J. E. T., Hodell, D. A., Singer, B. S., Xuan, C.: Reconciling Astrochronological and 40Ar/39Ar Ages for the Matuyama-Brunhes Boundary and Late Matuyama Chron, Geochem., Geophys., Geosyst., 11 (12), https://doi.org/10.1029/2010GC003203, 2010.

Conroy, J. L., Cobb, K. M., Lynch-Stieglitz, J., Polissar, P. J.: Constraints on the Salinity–Oxygen Isotope Relationship in the Central Tropical Pacific Ocean, Mar. Chem., 161, 26–33, https://doi.org/10.1016/j.marchem.2014.02.001, 2014.

Dang, H., Wu, J., Xiong, Z., Qiao, P., Li, T., Jian, Z.: Orbital and Sea-Level Changes Regulate the Iron-Associated Sediment Supplies from Papua New Guinea to the Equatorial Pacific, Quat. Sci. Rev., 239, 106361, https://doi.org/10.1016/j.quascirev.2020.106361, 2020.

de Garidel-Thoron, T., Rosenthal, Y., Bassinot, F., Beaufort, L.: Stable Sea Surface Temperatures in the Western Pacific Warm Pool over the Past 1.75 Million Years, Nature, 433 (7023), 294–298. https://doi.org/10.1038/nature03189, 2005

de Garidel-Thoron, T., Rosenthal, Y., Beaufort, L., Bard, E., Sonzogni, C., Mix, A. C.: A Multiproxy Assessment of the Western Equatorial Pacific Hydrography during the Last 30 Kyr, Paleoceanogr., 22 (3). https://doi.org/10.1029/2006PA001269, 2007.

Heaton, T. J., Köhler, P., Butzin, M., Bard, E., Reimer, R. W., Austin, W. E. N., Ramsey, C. B., Grootes, P. M., Hughen, K. A., Kromer, B., Reimer, P. J., Adkins, J., Burke, A., Cook, M. S., Olsen, J., Skinner, L. C.: Marine20—The Marine Radiocarbon Age Calibration Curve (0–55,000 Cal BP), Radiocarbon, 62 (4), 779–820, https://doi.org/10.1017/RDC.2020.68, 2020.

Hobart, B., Lisiecki, L.E., Rand, D., Lee, T., Lawrence, C. E.: Late Pleistocene 100-kyr glacial cycles paced by precession forcing of summer insolation, Nat. Geosci., https://doi.org/10.1038/s41561-023-01235-x, 2023.

Holbourn, A., Kuhnt, W., Kawamura, H., Jian, Z., Grootes, P., Erlenkeuser, H., Xu, J.: Orbitally paced paleoproductivity variations in the Timor Sea and Indonesian Throughflow variability during the last 460 Kyr, Paleoceanogr., 20 (3), https://doi.org/10.1029/2004PA001094, 2005.

Hollstein, M., Mohtadi, M., Kienast, M., Rosenthal, Y., Groeneveld, J., Oppo, D. W., Southon, J. R., Lückge, A. The Impact of Astronomical Forcing on Surface and Thermocline Variability Within the Western Pacific Warm Pool Over the Past 160 Kyr, Paleoceanogr. and Paleoclimatol., 35 (6), e2019PA003832, https://doi.org/10.1029/2019PA003832, 2020.

Huybers, P., Wunsch, C.: A Depth-Derived Pleistocene Age Model: Uncertainty Estimates, Sedimentation Variability, and Nonlinear Climate Change, Paleoceanogr., 19 (1), https://doi.org/10.1029/2002PA000857, 2004.

Imbrie, J., Hays, J. D., Martinson, D. G., McIntyre A., Mix A. C., Morley, J. J., Pisias N. G., Prell, W. L., and Shackleton, N. J.: The orbital theory of Pleistocene climate: Support from a revised chronology of the marine δ18O record, Milankovitch and Climate, Part 1, D. Reidel Publishing Company, Dordrecht, Netherlands, 269 pp., ISBN 9027717915, 1984.

Jian, Z., Wang, Y., Dang, H., Mohtadi, M., Rosenthal, Y., Lea, D. W., Liu, Z., Jin, H., Ye, L., Kuhnt, W., Wang, X.: Warm Pool Ocean Heat Content Regulates Ocean–Continent Moisture Transport, Nature, 612 (7938), 92–99, https://doi.org/10.1038/s41586-022-05302-y, 2022.

Lee, T., Rand, D., Lisiecki, L. E., Gebbie, G., Lawrence, C. E.: Bayesian Age Models and Stacks: Combining Age Inferences from Radiocarbon and Benthic $d^{18}O$ Stratigraphic Alignment, EGUsphere, 1–29, https://doi.org/10.5194/egusphere-2022-734, 2022 (accepted for publications at Clim. Past)

Lea, D. W.: The 100,000-Yr Cycle in Tropical SST, Greenhouse Forcing, and Climate Sensitivity, American Meteorological Society: J. Clim., 17 (11), 2170–2179, https://doi.org/10.1175/1520-0442(2004)017<2170:TYCITS>2.0.CO;2, 2004.

Lea, D. W., Pak, D. K., Spero, H. J.: Climate Impact of Late Quaternary Equatorial Pacific Sea Surface Temperature Variations, Science, 289 (5485), 1719–1724, https://doi.org/10.1126/science.289.5485.1719, 2000.

Li L., Li, Q., Tian, J., Wang, P., Wang, H., Liu, Z.: A 4-Ma record of thermal evolution in the tropical western Pacific and its implications on climate change, Earth and Planet. Sci. Lett.,, 309, 10-20, doi.org/10.1016/j.epsl.2011.04.016, 2011.

Li, Z.; Shi, X., Chen, M.-T.; Wang, H., Liu, S., Xu, J., Long, H., Troa, R. A., Zuraida, R., Triarso, E.: Late Quaternary Fingerprints of Precession and Sea Level Variation over the Past 35 Kyr as Revealed by Sea Surface Temperature and Upwelling Records from the Indian Ocean near Southernmost Sumatra, Quat. Int., 425, 282–291. https://doi.org/10.1016/j.quaint.2016.07.013, 2016.

Linsley, B. K., and M. T. von Breymann: Stable isotopic and geochemical record in the sulu sea during the last 750 k.y.:Assessment of surface water variability and paleoproductivity changes, Proceedings of the Ocean Drilling Program, Scientific Results, 24, 379-396, https://doi.org/10.2973/odp.proc.sr.124.151.1991,1991.

Linsley, B., Rosenthal, Y., Oppo, D.: Holocene Evolution of the Indonesian Throughflow and the Western Pacific Warm Pool, Nat. Geosci., 3, https://doi.org/10.1038/ngeo920, 2010.

Lisiecki, L. E., Raymo, M. E.: A Pliocene-Pleistocene Stack of 57 Globally Distributed Benthic δ18O Records, Paleoceanogr., 20 (1), https://doi.org/10.1029/2004PA001071, 2005.

Lisiecki, L. E., Stern, J. V.: Regional and Global Benthic Δ18O Stacks for the Last Glacial Cycle, Paleoceanogr., 31 (10), 1368–1394, https://doi.org/10.1002/2016PA003002, 2016.

Lo, L., Chang, S.-P., Wei, K.-Y., Lee, S.-Y., Ou, T.-H., Chen, Y.-C., Chuang, C.-K., Mii, H.-S., Burr, G. S., Chen, M.-T., Tung, Y.-H., Tsai, M.-C., Hodell, D. A., Shen, C.-C.: Nonlinear Climatic Sensitivity to Greenhouse Gases over Past 4 Glacial/Interglacial Cycles, Sci Rep, 7 (1), 4626, https://doi.org/10.1038/s41598-017-04031-x, 2017.

Locarnini, R. A., Mishonov, A. V., Baranova, O. K., Boyer, T. P., Zweng, M. M., Garcia, H. E., Reagan, J. R., Seidov, D., K. Weathers, Paver, C. R., and Smolyar, I.: Temperature, World Ocean Atlas 2018, NOAA Atlas NESDIS 81 [data set], https://archimer.ifremer.fr/doc/00651/76338/, 2019.

Oppo, D. W., Linsley, B. K., Rosenthal, Y., Dannenmann, S., Beaufort, L.: Orbital and Suborbital Climate Variability in the Sulu Sea, Western Tropical Pacific, Geochem., Geophys., Geosyst., 4 (1), 1–20, https://doi.org/10.1029/2001GC000260, 2003.

Regoli, F., de Garidel-Thoron, T., Tachikawa, K., Jian, Z., Ye, L., Droxler, A. W., Lenoir, G., Crucifix, M., Barbarin, N., Beaufort, L.: Progressive Shoaling of the Equatorial Pacific Thermocline over the Last Eight Glacial Periods, Paleoceanogr., 30 (5), 439–455, https://doi.org/10.1002/2014PA002696, 2015.

Rosenthal, Y., Oppo, D. W., Linsley, B. K.: The Amplitude and Phasing of Climate Change during the Last Deglaciation in the Sulu Sea, Western Equatorial Pacific, Geophys. Res. Lett., 30 (8). https://doi.org/10.1029/2002GL016612, 2003

https://doi.org/10.5194/essd-2023-335
Preprint. Discussion started: 24 August 2023

Sadekov, A., Eggins, S. M., De Deckker, P., Ninnemann, U., Kuhnt, W., Bassinot, F.: Surface and Subsurface Seawater Temperature Reconstruction Using Mg/Ca Microanalysis of Planktonic Foraminifera Globigerinoides Ruber, Globigerinoides Sacculifer, and Pulleniatina Obliquiloculata, Paleoceanogr., 24 (3), https://doi.org/10.1029/2008PA001664, 2009.

Shakun, J. D., Lea, D. W., Lisiecki, L. E., Raymo, M. E.: An 800-Kyr Record of Global Surface Ocean δ18O and Implications for Ice Volume-Temperature Coupling, Earth and Planet. Sci. Lett.,, 426, 58–68, https://doi.org/10.1016/j.epsl.2015.05.042, 2015.

Singer, B. S.: A Quaternary Geomagnetic Instability Time Scale, Quat. Geochronol., 21, 29–52, https://doi.org/10.1016/j.quageo.2013.10.003, 2014.

Spero, H. J., Mielke, K. M., Kalve, E. M., Lea, D. W., Pak, D. K.: Multispecies Approach to Reconstructing Eastern Equatorial Pacific Thermocline Hydrography during the Past 360 Kyr, Paleoceanogr., 18 (1), https://doi.org/10.1029/2002PA000814, 2003.

Spratt, R. M., Lisiecki, L. E. A Late Pleistocene Sea Level Stack, Clim. Past, 12 (4), 1079–1092, https://doi.org/10.5194/cp-12-1079-2016, 2016.

Tachikawa, K., Timmermann, A., Vidal, L., Sonzogni, C., Timm, O. E.: CO2 Radiative Forcing and Intertropical Convergence Zone Influences on Western Pacific Warm Pool Climate over the Past 400ka, Quat. Sci. Rev., 86, 24–34, https://doi.org/10.1016/j.quascirev.2013.12.018, 2014.

Visser, K., Thunell, R., and Stott, L.: Magnitude and Timing of Temperature Change in the Indo-Pacific Warm Pool during Deglaciation, Nature, 421, 152–155. https://doi.org/10.1038/nature01297, 2003.

Wang, L.: Isotopic Signals in Two Morphotypes of Globigerinoides Ruber (White) from the South China Sea: Implications for Monsoon Climate Change during the Last Glacial Cycle, Paleoceanogr., Palaeoclimatol., Palaeoecol., 161 (3), 381–394, https://doi.org/10.1016/S0031-0182(00)00094-8, 2000.

Xu, J., Holbourn, A., Kuhnt, W., Jian, Z., Kawamura, H.: Changes in the Thermocline Structure of the Indonesian Outflow during Terminations I and II, Earth and Planet. Sci. Lett., 273 (1), 152–162, https://doi.org/10.1016/j.epsl.2008.06.029, 2008.